The role of groundwater in CO2 production and carbon storage in Mediterranean peatlands: A geochemical approach

S. Santoni, E. Garel, M. Gillon, M. Babic, J.E. Spangenberg, B. Bomou, D. Sebag, T. Adatte, R. van Geldern, V. Pasqualini, A. Mattei, F. Huneau

PII: S0048-9697(22)08201-8

DOI: https://doi.org/10.1016/j.scitotenv.2022.161098

Reference: STOTEN 161098

To appear in: *Science of the Total Environment*

Received date: 28 July 2022

Revised date: 28 October 2022

Accepted date: 17 December 2022

Please cite this article as: S. Santoni, E. Garel, M. Gillon, et al., The role of groundwater in CO2 production and carbon storage in Mediterranean peatlands: A geochemical approach, *Science of the Total Environment* (2022), https://doi.org/10.1016/j.scitotenv.2022.161098

The role of groundwater in CO_2 production and carbon storage in Mediterranean peatlands: a geochemical approach

S. Santoni[1,2], E. Garel[1,2], M. Gillon[3], M. Babic[3], J. E. Spangenberg[4], B. Bomou[5], D. Sebag[6], T. Adatte[5], R. van Geldern[7], V. Pasqualini[1,2], A. Mattei[1,2], F. Huneau[1,2]

[1]Université de Corse Pascal Paoli, Département d'Hydrogéologie, Campus Grimaldi, BP52, 20250 Corte, France.
[2]CNRS, UMR 6134 SPE, BP52, 20250 Corte, France.
[3]Avignon Université, UMR 1114 EMMAH, INRAE, 301 rue Baruch de Spinoza, BP21239, 84916 Avignon, France.
[4]University of Lausanne, Institute of Earth Surface Dynamics (IDYST), Géopolis, 1022 Chavannes-près-Renens, Lausanne 1015, Switzerland.
[5]University of Lausanne, Institute of Earth Sciences (ISTE), Géopolis, 1022 Chavannes-près-Renens, Lausanne 1015, Switzerland.
[6]IFP Energies Nouvelles, Earth Sciences and Environmental Technologies Division, 1-4 Avenue du bois Préau, 92852 Rueil-Malmaison, France
[7]Friedrich-Alexander-Universität Erlangen-Nürnberg, Department of Geography and Geosciences, GeoZentrum Nordbayern, Schlossgarten 5, 91054 Erlangen, Germany.

Corresponding author
Sebastien Santoni : santonisebastien17@gmail.com ; santoni_s@univ-corse.fr

ORCID numbers:
S. Santoni: 0000-0003-0817-2811, **E. Garel**: 0000-0002-8014-6805, **M. Gillon**: xx, **M. Babic**: 0000-0001-9306-1870, **J.E. Spangenberg**: 0000-0001-8636-6414, **B. Bomou**: 0000-0002-7600-5276, **D. Sebag:** 0000-0002-6446-6921, **T. Adatte**: 0000-0002-4319-2212, **R. van Geldern**: 0000-0003-2786-2893, **V. Pasqualini**: 0000-0001-5919-4805, **A. Mattei**: 0000-0002-4262-4079, **F. Huneau**: 0000-0002-8014-6805.

The role of groundwater in CO_2 production and carbon storage in Mediterranean peatlands: an isotope geochemistry approach

Abstract

Peatlands are permanent wetlands recognized for ecosystem services such as biodiversity conservation and carbon storage capacity. Little information is available about their response to global change, the reason why most Earth system climate models consider a linear increase in the release of greenhouse gases (GHG), such as CO_2, with increasing temperatures. Nevertheless, numerous studies suggest that an increase in the temperature may not imply a decrease in photosynthesis and carbon storage rates if water availability is sufficient, the latter being under the control of local hydrology mechanisms. Mediterranean peatlands well illustrate this fact. Since they are groundwater-dependent, they are hydrologically resilient to the strong seasonality of hydroclimatic conditions, especially during the summer drought. In the present study, we demonstrate that, even if such peatlands release CO_2 into the atmosphere, they can maintain a carbon storage capacity. To this end, a geochemical study disentangles the origin and fate of carbon within a Mediterranean peatland at the watershed scale. Field parameters, major ions, dissolved organic and inorganic carbon content and associated $\delta^{13}C$ values allow for characterizing the seasonality of hydrochemical mechanisms and carbon input from an alluvial aquifer (where rain, river, shallow, and deep groundwater flows are mixing) to the peatland. The inorganic and organic content of peat soil and $\delta^{13}C$ values of total organic matter and CO_2 complete the dataset, making it possible to provide arguments in favour of lower organic matter oxidation compared to primary production. Overall, this study highlights the groundwater role in the fluxes of CO_2 at the peatland-atmosphere

interface, and more broadly the need to understand the interactions between the water and carbon cycles to build better models of the future evolution of the global climate.

Keywords (max 6)

Groundwater-dependent ecosystem, Origin of carbon; Peatland-carbon-water system; Peatland-atmosphere interface; Sources and sinks of carbon.

1. Introduction

Almost 1,000 Gt of carbon are stored in northern hemisphere peatland ecosystems such as boreal bogs, fens, and tundra wetlands (Gorham, 1991; Yu, 2012; Amesbury et al., 2019). Changes in peatland carbon balance could provide positive feedback to atmospheric forcing of climate if these ecosystems and their component organisms, mostly Sphagnum mosses, were affected by the global change effects (Robroek et al., 2009; Turetsky et al., 2012). However, peatlands are still underrepresented in the main Earth system models that compute future climate projections, considering only a systematic increase in the release of stored carbon as greenhouse gas with increasing temperatures due to organic matter oxidation induced by desiccation (Belyea and Malmer, 2004; Fenner and Freeman, 2011; Loisel et al., 2020).

Stringently, an increase in global temperatures does not systematically cause a decrease in the availability of water resources at a lower scale; local hydrology being the main driver of peatland water level variation (Wieder et al., 2007). However, although the peatland surface responds to increasing temperature, the stored organic carbon may be preserved under anoxic conditions, with methane and carbon dioxide being produced from the decomposition of actual surface-derived photosynthates (Wilson et al., 2016). Furthermore, Salimi et al. (2021) show in experiments reproducing temperature increases that peatlands mesocosms can also act as carbon sinks, even without any water level management strategy. These results are in agreement with previous studies suggesting that even if maximum sphagnum photosynthetic rates decline rapidly with drought and desiccation, high photosynthetic rates may be maintained in wet conditions at temperatures up to 30 °C or higher (Weston et al., 2015). Therefore, there is a need to learn more about possible changes in the carbon storage function of peatlands by taking into account the complex links within the peatland-carbon-water system to better constrain future climate projections.

Even if the Mediterranean area is characterized by a strong seasonality of hydroclimatic conditions with warm and dry summers, peatlands are small and scattered (Fig. 1A). They represent up to 42% of the total wetland surface (Parish et al., 2008; Gardner and Finlayson, 2018). Information on the carbon balance state of such natural peatlands under strong hydroclimatic pressures and located in a climate change hotspot remain scarce although it could provide decisive information with a head start on possible changes in the carbon stocks on a global scale. Recent studies have shown that the existence of peatlands in the Mediterranean context can be explained by the contribution of several surface and groundwater sources maintaining stable water levels over seasons (Charman, 2009; Santoni et al., 2021). As suggested earlier, Sphagnum photosynthesis seems then possible in the context of warming climate but it remains to be seen whether the carbon storage is effective under natural conditions. In particular, it appears necessary to understand how the seasonality of surface and groundwater inputs influences the primary production and the level of anoxia, ensuring carbon stock preservation. In addition, recharge water coming from the catchment constitutes also a potential external source of carbon (e.g., carbonate dissolution, soil respiration) that should be estimated to understand the carbon fluxes observed at the peatland-atmosphere interface.

In this study, we attempt to determine the status of the carbon balance of Mediterranean peatlands by using a selection of tools from isotope hydrology and geochemistry, well adapted to document the interactions of the water and carbon cycles (Appelo and Postma, 2004; Clark and Fritz, 2013; Jasechko, 2019; Baudin et al., 2021). These tools will be tested on the Moltifau pilot site located in Corsica, a French Mediterranean island with well-documented hydrogeology. Within an alpine watershed at medium altitude, with cold, wet winters and hot, dry summers, this pilot site is able to illustrate the evolution of northern peatlands because the hydroclimatic context is very unfavourable to its preservation. Then, based on an innovative natural multi-tracing experiment organized around four quarterly field campaigns in contrasting hydrological conditions, this study has several objectives. First will be characterized the seasonality of the peatland hydrochemical processes. Next, dissolved inorganic carbon (DIC) input from the alluvial aquifer to the peatland will be evaluated using the DIC carbon isotope compositions ($\delta^{13}C$ values) and the mixing proportions of rain, river, soil water, and groundwater, as shown by Santoni et al. (2021). Then, pathways of CO_2 production and carbon storage capacity will be elucidated by referring to the carbon content as dissolved inorganic, organic and total carbon (DIC, DOC, and TOC) and their $\delta^{13}C$ values in water, peat organic matter, soil and CO_2 emissions at the peatland-atmosphere interface. Additionally, peat CHN content, Rock-Eval® thermal analysis, and mineralogy will be discussed. Finally, the new results will give insights into the relevance of isotope hydrology and geochemistry to disentangle the interactions between the water and carbon cycles, focusing on the groundwater role in the fluxes of CO_2 at the peatland-atmosphere interface.

2. Material and method

2.1. Study site

The Moltifau peatland (Fig. 1B) is a pilot site selected for its strategic location in the mountainous Mediterranean Island of Corsica (France). According to the Köppen-Geiger climate classification, Corsican coasts are categorized in a Csa climate, mid-mountains in a Csb climate, and small areas of high altitude in a subarctic Dfc climate. Such a hydroclimatic context implies strong inter-seasonal and inter-annual heterogeneity in temperature and rainfall records (Peel et al., 2007).

Biological inventories have revealed a great diversity at the Mediterranean scale, characterised by rare fauna and flora including three species of Sphagnum moss (Sphagnum papillosum, Sphagnum subnitens, Sphagnum centrale), an orchid (Liparis loeselii), four reptile species (including the European pond turtle Emys orbicularis) and an endemic amphibian (Salamandra corsica). The Moltifau peatland is part of the Natura 2000 network and is recognised as a wetland of international importance by the RAMSAR convention (Burguet-Moretti, 2011). It is referenced as an acidic and young raised bog (^{14}C dating to 515 ± 45 a) by Reille (1997). Although some residues remain from past landfill activities in the area, the peatland itself can be considered "pristine” (Poher, 2017).

The Moltifau peatland, which lies on an alluvial plain between 240 and 270 m asl, extends over 40,000 m² within the Ascu River valley (Fig. 1C). This valley defines an alpine watershed extending over 365 km² and reaching an elevation of 2706 m asl. The Ascu River displays a torrential Mediterranean pluvio-nival regime with a mean annual flow of 5.1 m^3 s$^{–1}$ (from 0.8 m^3 s$^{–1}$ to 8.9 m^3/s in summer and fall, respectively). The Ascu River regime is also influenced by the high altitude Dfc climate, involving contribution of spring snowpack melting to the flow. However, the Moltifau peatland location at low altitude implies a Csb climate including severe summer drought conditions. The mean annual temperature is 14.4 °C (from 25 °C in summer to 4 °C in winter), and the average rainfall amount is 726 mm y$^{–1}$ (from 13 to 99 mm in summer and fall, respectively) for the 1990-2020 period.

According to Genevier (2014), the Moltifau peatland lies on sedimentary deposits covering well-fractured, pink perthitic granites extending in surface as an 820 m asl elevation massif. The alluvial sediments are more or less altered pebbles, nested in a clayey grey sandy matrix close to the riverbed and orange paleosol close to the piedmont, both are organized in terraces of different ages with a thickness of up to several tens of meters. Alluvial material permeability is about 6.4 × 10$^{−4}$ m s$^{–1}$. Colluvium resulting from the granite massif erosion accumulates on its piedmont until the alluvial plain in the south of the peatland to a thickness of a few meters. An alder forest surrounding the peatland hosts tiny temporary streams supplied by runoff from the granite massif and numerous springs on the ground supplied by subsurface flows from the colluvium.

The river flow and the alluvial aquifer water level are strongly correlated with the monthly rainfall amount. Highest values correspond to Fall and Winter flood seasons, the lowest ones to the Summer baseflow. The water level in the peatland follows the same pattern but in a much more dampened way: flood events cause slight increases in the peatland water table, only about ten centimetres maximum for a few days. Thus, the peatland is interpreted to be recharged upstream by the alluvial groundwater discharge due to a topographic threshold affecting the alluvium terraces

(Genevier, 2014; Santoni et al., 2021). Despite the stability of the peatland water level, the recharge contributions of diverse water sources vary significantly over the seasons. An endmember mixing analysis based on isotope hydrology tools and hydrochemistry indicates that during fall-winter, peatland is mainly recharged by the rainfall, the Ascu River, and subsurface colluvium flows. During spring-summer, water supply is mostly provided by the Ascu River, the subsurface and the deep groundwater flows from the underlying fractured granite. These recharge flows and subsequent mixing processes within the alluvial aquifer as well as within the peatland have been quantified for each season in space by Santoni et al. (2021).

Overall, alluvial aquifer-peatland interaction appears more under the influence of surface water upstream and of groundwater downstream (Santoni et al., 2021). Thus, according to Charman (2009), the Moltifau peatland classification can be defined more accurately as a raised mire (ombrotrophic bog) and sloping mire (minerotrophic fen) in the same direction. Also, from the alluvial sediments to the top of the peatland, the soil log displays up to 2 m of sand and organic matter, 0.2 m of silts and organic matter, and up to 1 m of roots, wood, and plant debris (Poher, 2017). The peatland being in continuity with the underlying alluvial aquifer, with a water level close to the surface, the acrotelm can be neglected. All the peat log can be considered as a catotelm (Genevier, 2014; Santoni et al., 2021).

2.2. Field and laboratory procedures

Four quarterly field surveys were conducted under contrasting hydrological conditions to characterize a complete hydrological cycle in June 2019 for the spring, August 2018 for the summer, December 2019 for the fall, and February 2019 for the winter season. Since the peatland is recharged by an alluvial aquifer where river, shallow, and deep groundwater are mixing together, a network of 24 sampling points was developed. This latter includes 5 peatland piezometers (T1, T2, T4, T5, T6, from 0,7 to 1,2 m deep), 3 peatland outlet runoff sites (R1, R5, R6), 9 alluvial aquifer boreholes and springs spread all around the peatland (F1, F2, F3, F4, F5, F7, F8, R17, R19 up to 6 m deep), 3 colluvium soil subsurface springs within the alder forest surrounding the peatland (R11, R12), 1 borehole reaching deep groundwater within the well fractured granitic massif (F6, 99 m deep), and 5 river sampling sites downstream aside the peatland area (R7, R8, R18, R3).

Water physic-chemical parameters such as electrical conductivity (EC, μS cm^{-1}), temperature (T, °C), pH, redox potential (Eh, mV), and dissolved oxygen (DO, saturation percentage, %) were measured in the field with a WTW Cond 3310 meter (WTW GmbH, Weilheim, Germany). The alkalinity was also determined in the field using a Hach digital titrator (Hach Company, Loveland, USA). Groundwater sampling was performed after purging the piezometers and stabilization of the physic-chemical parameters. Samples for major ions (NO_3^-, Cl^-, SO_4^{2-}, Na^+, Ca^{2+}, Mg^{2+}, K^+) were filtered through 0.45 µm nitrocellulose membranes and collected in two 50 mL polyethylene bottles. One of the samples was acidified for cation analysis using ultrapure HNO_3. The ionic content was determined using a Dionex ICS 1100 chromatography (Thermo Fisher Scientific, Waltham, USA) at the Hydrogeology Department of the University of Avignon, France (HD-UAV). The analysis was considered valid for an ionic balance deviation of less than 5 %. DIC content was determined from field alkalinity and pH measurements according to Appelo and Postma (2004). The samples for DOC and TOC analysis were collected in two 50 mL polyethylene bottles, the one for DOC passed a 0.45 µm nitrocellulose membrane. The DOC and TOC analyses were performed using a TOC 700 analyzer (Bioritech

Industry, France) by removal of the DIC by acid treatment and then hot oxidation of the DOC to CO_2. The DIC, DOC, and TOC analyses were performed at HD-UAV. Samples for the carbon isotope analysis were prepared by extracting and purifying the CO_2 in a vacuum extraction line with cryogenic traps. The CO_2 from water samples was extract by acid etching, from soils by in situ vacuum extraction, and collected into chambers at the peatland-atmosphere interface. The carbon isotope compositions were reported in the delta ($\delta^{13}C$) notation as variation of the $^{13}C/^{12}C$ ratio in per mil vs Vienna Pee Dee Belemnite limestone (VPDB) standard. The $\delta^{13}C$ of the CO_2 fractions were measured at the HD-UAV using Thermo Fischer Scientific (Bremen, Germany) Delta S isotope ratio mass spectrometer. In both liquid and gas phases, the $\delta^{13}C$ standard error is less than 10%.

Peat soil organic matter amount and type as well as its mineralogy analysis were carried out on samples collected close to T1, T2, T4, T5, T6 at two levels of depth: in the lower part within the sand and organic matter layer, and in the upper part in the organic matter, roots, wood, and plant debris layer (see section 2.1. Study site). Peat total nitrogen and carbon abundances (%) were determined using a CHNS Flash EA 1112 elemental analyzer (Thermo Scientific, Milan, Italy) at the University of Lausanne (ISTE-UNIL), Switzerland. Analytical accuracy and precision were better than 0.01 and 0.1% for N and C contents, respectively. The type and amount of organic matter were determined at ISTE-UNIL using a Rock-Eval ® 6 thermal analysis device according to Espitalie et al. (1985) and Behar et al. (2001). The calculated parameters included TOC (wt.%), hydrogen index (HI, mg hydrocarbons g^{-1} TOC), oxygen index (OI, mg CO2 g^{-1} TOC), and temperature of maximum pyrolysis yield (T_{max}, ºC). The calibration was performed with the IFP 160000 standard (IFP, French Institute of Petroleum, Paris, France), with a precision better than 0.1%. The whole-peat mineralogy was determined by X-ray diffractometry (XRD) from homogenous <40 µm powders using a X-TRA Thermo-ARL Diffractometer (Thermo Fischer Scientific, Waltham, USA) according to the Kübler's procedure (Kübler, 1997) at ISTE-UNIL. The semi-quantitative estimation (in %) of the grain minerals had a precision of 5% and 5–10% for phyllosilicates. The files generated are transformed into calculated files by the software WinXRD 2.0-6 (ThermoFischer program, Lausanne) using a fast Fourier noise filter, background subtraction and Ka2 stripping. The measurements are usually made on calculated files. The peat organic carbon δ^{13}C values were determined in decarbonated samples using an elemental Carlo Erba 1108 EA analyzer (Fisons Instruments, Milan, Italy) connected to a Delta V Plus isotope ratio mass spectrometer (Thermo Fischer Scientific, Bremen, Germany) at the IDYST-UNIL, following procedures described previously (Spangenberg and Zufferey, 2018).

All the data produced in the framework of the present study are available online (Santoni et al., 2022).

3. Results and discussion

3.1. Seasonality of the peatland hydrochemical processes

As several water sources contribute differently to the peatland recharge over the seasons, it appears necessary to understand the impact this may have on the peatland's hydrochemical processes.

The temperature of alluvial groundwater and peatland water follows the seasonality of hydroclimatic conditions (Fig. 2). However, no significant differences appear between these two water sources on a seasonal scale, that is consistent with the groundwater dependency of the studied peatland. The trend is different for the EC for which no significant difference is observed over the seasons and between the two water sources, except in summer. The summer higher values observed in the peatland may reflect peat oxidation and/or enhanced mineral phase weathering (Appelo and Postma, 2004). Indeed, even if the pH is stable over time within the peatland, the input of more acidic alluvial groundwater may favour the hydrolysis of mineral phases and ion liberation in peat water. Moreover, pH values are significantly higher and Eh values lower in the peatland compared to the alluvial groundwater, especially in summer. This suggests the predominance of reduction mechanisms, well-known to consume protons and cause water alkalinization while lowering Eh to negative values. This is consistent with the significant decrease in nitrate and sulphate levels observed in the peatland compared to the alluvial groundwater in summer. According to the Eh mean value around -21 mV in summer, chemical species such as NO_3^-, SO_4^{2-}, and HCO_3^- may be reduced to form NO_2^-, N_2, NH_4^+, H_2S and CH_4. Indeed, oxidation of hydrocarbons coupled with sulphate reduction in anaerobic environment increases the SO_4^{2-}/HCO_3^- ratio (Cassarini, 2018). Because not all SO_4^{2-} is reduced, CH_4 may be oxidized at such an Eh value. The lack of direct measurement of this gas in the field requires caution in this interpretation. However, significant O_2 levels under reducing conditions suggest a high production of this gas by peatland aquatic plants photosynthesis. This is supported by the significantly lower DIC, higher $\delta^{13}C_{DIC}$ value and DOC contents in peat water compared to alluvial groundwater in summer (Corbett et al., 2012). The absence of significant differences between the O_2 and HCO_3^- contents suggest continuous equilibration with the atmosphere, degassing being favoured by the increase in temperature during the summer season. Nevertheless, significantly low $\delta^{13}C_{DIC}$ values (around -20 ‰) in alluvial groundwater and in peat water samples suggest the predominance of respiration by microorganisms during the winter (Jasechko, 2019). Even if the DIC content is always higher than the DOC within the peatland, organic matter oxidation does not necessarily exceed photosynthesis. Indeed, several peatland internal and external processes can be a source of DIC, with the alluvial groundwater being a significant external source of DIC to the peatland. Therefore, it appears necessary to identify the origin of contents of the DIC to be able to evaluate the relative efficiency of CO_2 production or storage at the peatland-atmosphere interface.

Overall, peatland water and alluvial groundwater hydrochemical processes appear comparable in winter and well contrasted in summer. Autumn and spring are seasons that allow for a transition between these two extremes. This is in good agreement with piezometric data that shows a large influence of river flood in Fall/Winter and of other groundwater sources during the Summer on the alluvial aquifer supplying the peatland (see Fig. 1D and the section 2.1. Study site).

3.2. Carbon input from the alluvial aquifer to the peatland

The $\delta^{13}C_{DIC}$ patterns in stream water and groundwater may depend on the mixing of several terrestrial DIC sources such as carbonate dissolution, soil respiration in forested catchments, or peatland-related hydrochemical processes (van Geldern et al., 2015; Campeau et al., 2018). While the carbon balance of groundwater-dependent peatlands is expected to be influenced by terrestrial DIC inputs (Charman, 2009), to our knowledge, the effect of such DIC sources on the $\delta^{13}C_{DIC}$ patterns of peatland waters has never been reported. Thus, in the present section, we will seek to put in evidence and quantify the input of DIC through alluvial groundwater. This will help to better constrain the pathways of CO2 production perceptible at the peatland-atmosphere interface.

Considering negligible the influence of geogenic DIC sources (no carbonate rocks within the watershed) and according to the principle of mass conservation, the $\delta^{13}C_{DIC}$ value of Moltifau peatland water is expected to correspond to that of a mixture of rainwater, colluvium springs, granite groundwater, and river water sources (all being collected and mixed within the alluvial aquifer supplying the peatland) in proportion given by Santoni et al. (2021). Mixing proportions of all peatland recharge components known, it is possible to apply a "reverse" end-member mixing analysis to define the theoretical $\delta^{13}C_{DIC}$ value in peat water and compare it to the measured one. Similar measured and computed data would highlight the watershed influence on peatland carbon content, different ones would suggest the presence of other processes driving the $\delta^{13}C_{DIC}$ values in peat water. According to Carrera et al. (2004), a reverse end-member mixing model can be expressed as follows:

$$1 = f_a + f_b + f_c + f_d \quad (1)$$

where f refers to the relative fraction, subscripts a, b, c, and d refers to the end-members including rainwater, colluvium, granite, and river.

$$[\delta^{13}C_{DIC}]_{\text{modeled}} = f_a \times [\delta^{13}C_{DIC}]_{\text{rainwater}} + f_b \times [\delta^{13}C_{DIC}]_{\text{colluvium}} + f_c \times [\delta^{13}C_{DIC}]_{\text{granite}} + f_d \times [\delta^{13}C_{DIC}]_{\text{river}} \quad (2)$$

This mixing model can be considered valid if the difference between the measured $\delta^{13}C_{DIC}$ value and the computed one is lower than the standard deviation coming from mixing rates estimates and $\delta^{13}C_{DIC}$ measurement (Table 1).

The mixing model match the measured $\delta^{13}C_{DIC}$ values in peatland water samples mainly in fall and winter (almost 65 % of the data). This suggests that groundwater DIC flows through the peatland without any further carbon isotope fractionation. By contrast, the mixing model does not always reproduce the measured $\delta^{13}C_{DIC}$ values in spring and summer (almost 35 % of the data). The difference between the measured and the computed $\delta^{13}C_{DIC}$ values suggests a contribution of source(s) of DIC with high $\delta^{13}C$. This result agrees with the $\delta^{13}C_{DIC}$ pattern observed in Fig. 2, showing somewhat higher $\delta^{13}C_{DIC}$ values in peat water during summer and to a lesser extent, during spring and fall.

3.3. Carbon production within the peatland

Soil-derived CO_2 by respiration (heterotrophic and/or autotrophic) and subsequent transport as DIC in river, subsurface, and ground waters are external sources of carbon for Mediterranean peatlands. However, many additional processes involving liquid and gas phases of the carbon cycle may take place within peatlands. Carbon uptake as CO_2 or DIC occurs during plant photosynthesis, the latter being the preferred carbon form fixed by Sphagnum (Charman, 2009). Peat accumulation is the most obvious result of the peatland carbon cycle, i.e., a balance between plant productivity and decomposition. The released DO by rooted vascular plants may allow CO_2 production by aerobic respiration, which can also be promoted by nitrate and sulphate reduction (Vile et al., 2003; Chanton et al., 2008). In addition, CO_2 could be released by aerobic respiration if the peat water level decreases. In deeper anaerobic layers, the CO_2 can be reduced to CH_4 while organic matter may be mineralized by methanogens to produce CO_2 and CH_4. The CH_4 can be oxidized to CO_2 before reaching the surface. Thus, CO_2 and CH_4 can be released to the atmosphere as gases or dissolved in water in runoff and groundwater (Corbett et al., 2012). In the following sections, the balance between all these processes will be discussed to find arguments to status on the peatland role as source or sink of greenhouse gases.

3.3.1. Respiration and evasion to the atmosphere

Usually, the water pH and alkalinity are the main drivers of the variability of $\delta^{13}C_{DIC}$ values due to the carbon isotope fractionations in the CO_2-DIC-carbonate system (Clark and Fritz, 2013). In acidic freshwater, such isotopic fractionation may be negligible. The CO_2 evasion fluxes and the peatland internal processes influence the DIC carbon isotope composition (Campeau et al., 2018). The Keeling and Miller-Tans plot analysis is well-known to constrain the $\delta^{13}C$ values of DIC sources (Keeling, 1958; Miller and Tans, 2003). Thus, we seek here to highlight the presence of dissolved carbon produced by the respiration of microorganisms as well as its evasion to the atmosphere.

The Keeling plot relies on CO_2 content and associated $\delta^{13}C_{CO2}$ values at the peatland-atmosphere interface while the Miller-Tans plot relies on DIC content and associated $\delta^{13}C_{DIC}$ values in peat water. In the latter, the slope of the regression lines corresponds to the $\delta^{13}C$ of the DIC source. Both analyses assume the principle of mass conservation, and the mixing of isotopically distinct carbon sources without any further fractionation.

In the Keeling plot, the Moltifau peatland CO_2 samples lie between soil, atmosphere, and an unknown source end member (Fig. 3A). This observation reveals the influence of soil respiration and CO_2 degassing combined with a source with higher $\delta^{13}C_{DIC}$ value as suggested by the mixing model (Table 1). In the Miller-Tans plot analysis, all the slopes display a highly significant linear relationship for the alluvial groundwater and peat water $\delta^{13}C_{DIC}$ values (Figs. 3B, and C). The $\delta^{13}C_{DIC}$ of the source is comparable for alluvial groundwater and peatland water during the winter and spring seasons, values are between -18.4 ‰ and -16.2 ‰. This result point to a negligible influence of internal peatland hydrochemical processes on $\delta^{13}C_{DIC}$ values of peat water signature as suggested by the mixing model (Table 1). The $\delta^{13}C$ of the DIC source is more enriched for peatland water compared with alluvial groundwater in fall and summer, with a maximal value of about –12.0 ‰ (Fig. 3C). This $\delta^{13}C$ value suggest that the peatland hydrochemical processes play an important role in the carbon isotope ratios of the DIC in peat water samples during these seasons.

3.3.2. Organic matter oxidation

The aim here is to identify the origin of carbon at the peatland-atmosphere interface, not coming from the catchment area thanks to groundwater, but from the *in situ* degradation of the peat organic matter. The latter would then indicate a loss of the carbon storage function of the peatland.

Methanogenesis is known to be the predominant mechanism of peatland organic matter mineralization (Romanowicz et al., 1995; Chasar et al., 2000). It consists of degradation of high-molecular weight organic matter (HMW-OM) in CO_2 and CH_4 (Corbett et al., 2012). A low temperature will favour the acetoclastic methanogenesis, whereas a low pH is advantageous to the hydrogenotrophic pathway (Kotsyurbenko et al., 2019). Methanogenesis leads to ^{13}C-enriched CO_2 and ^{13}C-depleted CH_4 compared to the HMW-OM (Corbett et al., 2012). The weighted mean of the $\delta^{13}C$ values of CO_2 and CH_4 correspond to the $\delta^{13}C_{HMW-OM}$. Such fractionation could explain the input of enriched $\delta^{13}C_{DIC}$ in peatland water of the present study. Nevertheless, both the acetoclastic and hydrogenothrophic pathways are well known to modify the hydrogen isotope composition of peatland water (δ^2H_w) (Corbett et al., 2012). The water oxygen isotope composition ($\delta^{18}O_w$) may also be affected, because during anaerobic degradation of organic matter, DO is utilized in carbon dioxide and methane production, the latter regulated by acetoclastic and hydrogenotrophic pathways (e.g., Kotsyurbenko et al, 2004; Jian et al, 2018). Siegel et al. (2001) reported that during methanogenesis in peatlands the waters are enriched in the heavy H isotopes. This may result in a positive offset of peatland water samples from the local $\delta^{2}H$ vs. $\delta^{18}O$ meteoric water line. In addition, the authors reported that methane flux rates measured at the peatland-atmosphere interface are systematically lower than the deeper methane production estimated by isotopic mass balance calculations. The determination of $\delta^{2}H_{w}$ and $\delta^{18}O_{w}$ is consequently a relevant tool to detect methanogenesis in peatlands. According to Santoni et al. (2021), all peatland water samples lie along the western Mediterranean and local meteoric water lines. This suggest a negligible methanogenesis (and subsequent oxidation) even if the three predominant Sphagnum species (ie. S. papillosum, S. subnites, and S. centrale) support methanogenesis (Larmola et al., 2010). Such observation remains consistent with the measured Eh (Fig. 2) as well as with the very low fluxes of methane observed in other similar natural peatlands worldwide (Abdalla et al., 2016).

The oxidative degradation of HMW-OM components may produce low-molecular weight organic matter (LMW-OM) compounds and CO_2 by anaerobic microbial respiration/oxidation using electron acceptors (e.g., oxygen, nitrate, manganese(IV), iron(III), sulfate, carbonate, humic compounds) (Lovley et al., 1996; Keller and Bridgham, 2007). If the reaction is complete, such mineralisation mechanisms generally cause any carbon isotope fractionation, the $\delta^{13}C$ value of the produced CO_2 is the same as the HMW-OM source (Corbett et al., 2012). Therefore, since the $\delta^{13}C_{HMW\text{-}OM}$ measured in the studied peatland range from –29.4 to –27.7 ‰ with a mean value about –28.65 ‰, the oxidation of organic compounds should lead to lower $\delta^{13}C_{DIC}$ values of peatland waters. This is not in agreement with the input of a

δ^{13}C source with -12.0 ± 0.6 ‰ suggested by the Miller-Tans plots. An explanation of this mismatch may be very limited oxidation of organic compounds in studied peatland environment.

To better understand the dynamics of organic matter, CHN contents and Rock-Eval® thermal analyses were performed on peat samples collected all over the Moltifau peatland at two deep levels (Figs. 1, 4). These analyses determine the TOC and inorganic carbon contents, and give insight into the type and maturation/decomposition stage of the organic matter (Sebag et al., 2006; Delarue et al., 2011). Specifically, the I-index quantifies the degree of transformation of fractions originating from biological material, while the R-index qualifies the thermally stable (i.e., refractory) fraction. From an I-Index vs R-Index diagram, Sebag et al. (2016) define three linear trends corresponding to the decomposition of biogenic compounds line ("humic"), to the "inherited" contributions from non-pedological processes, and a specific "spodic" trend coming from podzolization such as fulvic acids and aluminium. Besides, along with the decomposition line, they identify three areas corresponding to biological tissue as fresh plants remain, litter and organic horizons (i.e., poorly decomposed organic matter), and organo-mineral or mineral peat samples (i.e. highly decomposed organic matter). Therefore, these areas give a trend on the dynamics of storage or oxidation of organic matter.

The mineralogical composition of the peat samples is carbonate-free, and contains up to 2–37% quartz, 3–35% plagioclase, 3–30% K-feldspar, 12–20% phyllosilicates,0–3% goethite, and 0–2% pyrite. The non-quantified minerals vary between 1–74% and consist mainly of organic material (peat) and poorly crystallized minerals (e.g. clay minerals). The detrital fraction of these samples is consistent with the granitic lithology of the watershed. The mineralogy of the upper level samples

(Tx-U) is clearly relative to peatland with more than 66% of non-quantified minerals, 13–20% of phyllosilicates, low amount of detrital minerals as quartz, plagioclase and K-feldspar contents (>5% of each phase), and relatively enriched in goethite (2–3%). The mineralogy of the lower level samples (Tx-L) is characteristic of detrital alluvial deposits and mainly composed of quartz (20–37%), plagioclase (18–35%), K-feldspar (13–30%) and phyllosilicates (14–19%), and the non-quantified minerals content is relatively low (1–15%). Two samples sites (T4 and T5) exhibit the same mineralogical composition in the upper and lower parts, T4-U and L are characteristic to peatland composition and T5-U and L relative to detrital alluvial deposits. These mineralogical compositions are consistent with the TOC contents and suggest that the main part of the non-quantified minerals is relative to organic matter.

In the present study, peat samples display a wide range of carbon content (Figs. 4A, B). Samples from the lower level have the lower contents in both inorganic and organic carbon. With lower I-index values (around zero), samples T5-L and T2-L plots within the “organo-mineral and mineral horizons”, highlighting a slight trend in organic matter oxidation, especially in the lower part of the peatland (Fig. 4C). Indeed, at the peatland-alluvial aquifer interface, oxygenated groundwater flows through the peat, most probably creating locally favourable conditions for the oxidation of organic matter. However, most of the peat samples lie along the decomposition line, suggesting the decomposition of thermolabile biogenic compounds leading to an increase in the relative concentration of refractory organic compounds. Indeed, R-index values mainly range from 0.4 to 0.5 and plot within the “litters and organic horizons” field, indicating the prevalence of well-preserved or poorly decomposed organic matter. Moreover, samples from the upper level display a high organic carbon content including also, for some of them, a high inorganic fraction (T2-U and T6-U). Even if oxidation may occur in the upper level, this observation is consistent with high primary productivity within such an environment and argues in favour of effective carbon storage. This latter point is supported by the carbon isotope composition of the different carbon pools, as further discussed in the next paragraph.

3.3.3. Primary production

Photosynthesis and respiration are the main determinants of carbon balance in an ecosystem. These processes consume and produce CO_2, respectively, and their relative importance can be evaluated through the DIC, DOC, and O_2 contents in water. Respiration consumes DOC and O_2 to produce DIC while photosynthesis consumes DIC to produce DOC (and also particulate organic matter, POC) and O_2. In wetlands, these parameters can be influenced by redox conditions and temperature, and thus by seasonality of hydroclimatic conditions that triggers dissolution or degassing at the peatland-atmosphere interface. Moreover, the DIC is known to be depleted in ^{13}C by respiration, achieving $\delta^{13}C_{DIC}$ values ≈ –28 ‰, due to release of CO_2 from oxidation of organic compounds. The DIC is enriched in ^{13}C during photosynthesis, having $\delta^{13}C_{DIC}$ values ≈ 0 ‰ or higher), and around –9 ‰ in the atmosphere (Clark and Fritz, 2013). Thus, the DIC, DOC, and O_2 contents combined with their $\delta^{13}C$ values allow to evaluate the relative importance of respiration, exchange and isotopic equilibration with the atmosphere, and photosynthesis. Thus, in the present section, we will seek to understand if photosynthesis can explain the $\delta^{13}C$ source value, in order to add supplementary arguments in favour of the effective carbon storage function of such Mediterranean peatlands

In the settings of the present study, granite and alluvial groundwater display high DIC and low DOC contents. This is the opposite for river water, colluvium springs, peatland samples, and outlets (Fig. 5A). In addition, the O_2/DIC ratio and $\delta^{13}C_{DIC}$ signature are low for the alluvial groundwater samples, which is consistent with the heterotrophic respiration discussed previously (Table 1, Fig. 3). However, the $\delta^{13}C_{DIC}$ of granite groundwater is higher, suggesting rather an equilibration with the atmosphere kept during the recharge process (which is common for high altitudes, where soils are poorly developed and microbial activity limited). By contrast, the O_2/DIC ratios and $\delta^{13}C_{DIC}$ values in river water, colluvium springs, peatland, and outlets are high (while remaining under the influence of temperature and redox potential conditions). This observation argues in favour of a predominant photosynthesis process in the sampled areas (Fig. 5B). Note that the DOC content is highest in the colluvial springs and within the peatland compared with the river water, implying that primary production is higher in the peatland and the surrounding wetland.

Finally, photosynthesis constitutes a hydro-biogeochemical process that can explain the ^{13}C enrichment measured in the DIC of the peatland water samples. Indeed, considering an average $\delta^{13}C_{DIC}$ value in the alluvial groundwater of -20.2 ‰ and for the peat organic matter a $\delta^{13}C$ of -28.6 ‰, the photosynthetic fractionation would be -8.4 ‰. Therefore, the DIC in the peatland water is enriched in ^{13}C due to photosynthesis by 8.4 ‰ compared to the alluvial groundwater. Then, the $\delta^{13}C_{DIC}$ value in peatland water is expected to be close to -11.6 ‰ (Fig. 5B). This theoretical value is in agreement with the $\delta^{13}C_{DIC}$ value expected from the Miller-Tans plot (Fig. 3). Thus, the pathways of CO_2 production at the peatland-atmosphere interface are now fully detailed and constrained within the studied Mediterranean peatland.

4. Conclusion

The present study demonstrates the relevance of carbon isotope geochemistry to describe the pathways of CO_2 production at the peatland-atmosphere interface. In particular, this tool allows for the characterization of the hydrochemical process seasonality within the peatland. In winter, the low temperature of the groundwater supplying the peatland (connected upstream to a high-altitude mountain basin) limits the respiration of microorganisms despite the peatland oxygenation. In winter, but also in autumn and spring, CO_2 fluxes at the peatland-atmosphere interface are mainly influenced by groundwater fluxes coming from the alluvial aquifer. In summer, groundwater input from regional fractured granite massifs keep the peatland wet, primary production is high, and conditions are clearly reducing allowing then the preservation of produced organic matter. Indeed, the oxidation of organic matter has not been demonstrated, except in the deepest peat layer, in contact with the oxygenated groundwater of the alluvial aquifer. This was confirmed by analysing the organic and mineralogical content of the peat, as well as by the isotope signatures of peat organic matter, water, and CO_2 that are clearly under the influence of primary production.

This study highlights the role of groundwater, and more broadly the need to understand the interactions between the water and carbon cycles in determining the carbon balance of peatlands. We have thus been able to demonstrate that peatlands subjected to apparently unfavourable hydroclimatic conditions, as is the case in the Mediterranean, can rather maintain their carbon storage function. To understand the effects of climate change on high-latitude peatlands, which store the most carbon, it will therefore be necessary to be able to understand the evolution of their hydrogeological functioning. Groundwater flows can keep peatlands wet, and condition CO_2 flows at the peatland-atmosphere interface. High CO_2 fluxes do not necessarily mean organic carbon release but may also reflect the level of connection of a peatland with its watershed. Given the large carbon stock that peatlands represent around the world and the simplistic view of the carbon they are supposed to release in a warming climate, taking this new knowledge into account is necessary to build better models on the future evolution of the global climate.

Acknowledgements

The postdoctoral grant of Sébastien Santoni was financially supported by the Regional Council of Corsica “Culletivittà di Corsica”. This research is part of the GERHYCO interdisciplinary project dedicated to water management, ecology and hydro-ecosystem services in insular context. This research is also part of the Vienna International Atomic Energy Agency CRP F33027 project dedicated to isotopic assessment of the impacts of climatic and hydrological changes on wetland-groundwater ecosystem interactions. The authors would like to thank the Municipality of Moltifau for access to the peatland, and the French national forestry office “ONF” for their support to the implementation of the project. The authors would also like to thank the Moltifau inhabitants for access to their wells and boreholes during the field sampling.

References

Abdalla, M., Hastings, A., Truu, J., Espenberg, M., Mander, U. and Smith, P. 2016. Emissions of methane from northern peatlands: a review of management impacts and implications for future management options. Ecol Evol 6(19), 7080-7102. DOI : https://doi.org/10.1002/ece3.2469

Amesbury, M.J., Gallego-Sala, A. and Loisel, J. 2019. Peatlands as prolific carbon sinks. Nature Geoscience 12(11), 880-881. DOI: https://doi.org/10.1038/s41561-019-0455-y

Appelo, C.A.J. and Postma, D. 2004. Geochemistry, groundwater and pollution. DOI : https://doi.org/10.1201/9781439833544

Baudin, F., Tribovillard, N. and Trichet, J. 2021. Géologie de la matière organique. DOI: https://doi.org/10.1051/978-2-7598-2192-1

Behar, F., Beaumont, V. and Penteado, H.D.B. 2001. Rock-Eval© 6 technology: performances and developments. Oil & Gas Science and Technology 56(2), 111-134. DOI: https://doi.org/10.2516/ogst:2001013

Belyea, L.R. and Malmer, N. 2004. Carbon sequestration in peatland: patterns and mechanisms of response to climate change. Global Change Biology 10(7), 1043-1052. DOI: https://doi.org/10.1111/j.1529-8817.2003.00783.x

Burguet-Moretti, A., Petrera, C. and Culioli, J. 2011. Fiche descriptive sur les zones humide Ramsar (FDR), tourbière de Moltifao, Corse, France. RAMSAR 2009-2012 version. https://rsis.ramsar.org/ris/1994

Campeau, A., Bishop, K., Nilsson, M.B., Klemedtsson, L., Laudon, H., Leith, F.I., Öquist, M. and Wallin, M.B. 2018. Stable Carbon Isotopes Reveal Soil-Stream DIC Linkages in Contrasting Headwater Catchments. Journal of Geophysical Research: Biogeosciences 123(1), 149-167. DOI: https://doi.org/10.1002/2017JG004083

Carrera, J., Vázquez-Suñé, E., Castillo, O. and Sánchez-Vila, X. 2004. A methodology to compute mixing ratios with uncertain end-members. Water resources research 40(12). https://doi.org/10.1029/2003WR002263

Cassarini, C. 2018. Anaerobic oxidation of methane coupled to the reduction of different sulfur compounds in bioreactors. Geophysics [physics.geo-ph] HAL Id: tel-01743834. https://tel.archives-ouvertes.fr/tel-01743834

Chanton, J.P., Glaser, P.H., Chasar, L.S., Burdige, D.J., Hines, M.E., Siegel, D.I., Tremblay, L.B. and Cooper, W.T. 2008. Radiocarbon evidence for the importance of surface vegetation on fermentation and methanogenesis in contrasting types of boreal peatlands. Global Biogeochemical Cycles 22(4), n/a-n/a.10.1029/2008gb003274

Charman, D. 2009. Peat and peatlands. Earth Systems and Environmental Sciences, Encyclopedia of Inland Waters, pp 541-548.https://doi.org/10.1016/B978-012370626-3.00061-2

Chasar, L., Chanton, J., Glaser, P. and Siegel, D. 2000. Methane concentration and stable isotope distribution as evidence of rhizospheric processes: Comparison of a fen and bog in the Glacial Lake Agassiz Peatland complex. Annals of Botany 86(3), 655-663. DOI: https://doi.org/10.1006/anbo.2000.1172

Clark, I.D. and Fritz, P. 2013. Environmental isotopes in hydrogeology. CRC Press ISBN : 9780429069574, 342. DOI: https://doi.org/10.1201/9781482242911

Corbett, J.E., Tfaily, M.M., Burdige, D.J., Cooper, W.T., Glaser, P.H. and Chanton, J.P. 2012. Partitioning pathways of CO2 production in peatlands with stable carbon isotopes. Biogeochemistry 114(1-3), 327-340. DOI: https://doi.org/10.1007/s10533-012-9813-1

Delarue, F., Laggoun-Défarge, F., Disnar, J.-R., Lottier, N. and Gogo, S. 2011. Organic matter sources and decay assessment in a Sphagnum-dominated peatland (Le Forbonnet, Jura Mountains, France): impact of moisture conditions. Biogeochemistry 106(1), 39-52. DOI: https://doi.org/10.1007/s10533-010-9410-0

Espitalie, J., Deroo, G. and Marquis, F. 1985. Rock-Eval© pyrolysis and its applications (part one). Oil & Gas Science and Technology-Revue d'IFPEN 40(5), 563-579. DOI : https://doi.org/10.2516/ogst:1985035

Fenner, N. and Freeman, C. 2011. Drought-induced carbon loss in peatlands. Nature geoscience 4(12), 895-900. DOI: https://doi.org/10.1038/ngeo1323

Gardner, R.C. and Finlayson, C.M., et. al. 2018. Perspectives mondiales des zones humides: état des zones humides à l'échelle mondiale et des services qu'elles fournissent à l'humanité. . Secrétariat de la Convention de Ramsar Gland, Suisse. Link: https://www.ramsar.org/sites/default/files/documents/library/gwo_f.pdf

Genevier, M., Frissant, N., Tirmont, M., Auterives, C., Tissoux, H. and Bodéré, G. 2014. Tourbière de Valdu, Moltifao (2B) : structure, fonctionnement et sensibilité à l'érosion des berges de l'Asco. BRGM Rapport final BRGM/RP-63922-FR 1, 132(1), 132. http://infoterre.brgm.fr/rapports/RP-63922-FR.pdf

Gorham, E. 1991. Northern peatlands: role in the carbon cycle and probable responses to climatic warming. Ecological applications 1(2), 182-195

Jasechko, S. 2019. Global isotope hydrogeology—Review. Reviews of Geophysics 57(3), 835-965. DOI: https://doi.org/10.1029/2018RG000627

Joosten, H. 2009. The Global Peatland CO2 Picture: peatland status and drainage related emissions in all countries of the world. Wetlands International. https://www.wetlands.org/publications/the-global-peatland-co2-picture/

Keeling, C.D. 1958. The concentration and isotopic abundances of atmospheric carbon dioxide in rural areas. Geochimica et cosmochimica acta 13(4), 322-334.DOI: https://doi.org/10.1016/0016-7037(58)90033-4

Keller, J.K. and Bridgham, S.D. 2007. Pathways of anaerobic carbon cycling across an ombrotrophic-minerotrophic peatland gradient. Limnology and Oceanography 52(1), 96-107. DOI: https://doi.org/10.4319/lo.2007.52.1.0096

Kotsyurbenko, O., Glagolev, M., Merkel, A., Sabrekov, A. and Terentieva, I. 2019. Methanogenesis in soils, wetlands, and peat. Handbook of hydrocarbon and lipid microbiology Series. Biogenesis of hydrocarbons/AJM Stams and Diana Z. Sousa (Eds.) Springer-Verlag. Berlin Heidelberg. https://doi. org/10.1007/978-3-319-53114-4_9-1

Kübler, B. 1997. Concomitant alteration of clay minerals and organic matter during burial diagenesis. Soils and sediments, 327-357. DOI: https://doi.org/10.1007/978-3-642-60525-3_15

Larmola, T., Tuittila, E.-S., Tiirola, M., Nykänen, H., Martikainen, P.J., Yrjälä, K., Tuomivirta, T. and Fritze, H. 2010. The role of Sphagnum mosses in the methane cycling of a boreal mire. Ecology 91(8), 2356-2365.DOI: https://doi.org/10.1890/09-1343.1

Loisel, J., Gallego-Sala, A.V., Amesbury, M.J., Magnan, G. and Anshari, G.*e.a.* 2020. Expert assessment of future vulnerability of the global peatland carbon sink. Nature Climate Change 11(1), 70-77. DOI: https://doi.org/10.1038/s41558-020-00944-0

Lovley, D.R., Coates, J.D., Blunt-Harris, E.L., Phillips, E.J. and Woodward, J.C. 1996. Humic substances as electron acceptors for microbial respiration. Nature 382(6590), 445-448. DOI: https://doi.org/10.1038/382445a0

Miller, J.B. and Tans, P.P. 2003. Calculating isotopic fractionation from atmospheric measurements at various scales. Tellus B: Chemical and Physical Meteorology 55(2), 207-214.DOI: https://doi.org/10.3402/tellusb.v55i2.16697

Parish, F., Sirin, A., Charman, D., Joosten, H., Minaeva, T.Y. and Silvius, M. 2008. Assessment on peatlands, biodiversity and climate change. DOI: https://doi.org/10.1134/S207908641202003X

Peel, M.C., Finlayson, B.L. and McMahon, T.A. 2007. Updated world map of the Köppen-Geiger climate classification. Hydrology and earth system sciences 11(5), 1633-1644. DOI: https://doi.org/10.5194/hess-11-1633-2007

Poher, Y. 2017. Dynamique de la biodiversité et changements environnementaux en Corse depuis 7000 ans : éclairages paléoentomologiques et paléobotaniques. Thèse de Doctorat de l'Université d'Aix-Marseille. http://www.theses.fr/2017AIXM0435.

Reille, M. 1997. Analyse pollinique des tourbières de Valdo et Baghietto (commune de Moltifao, Haute-Corse). Rapport scientifique du programme Life, Office de l'environnement de la Corse, 8 pp.

Robroek, B.J., Schouten, M.G., Limpens, J., Berendse, F. and Poorter, H. 2009. Interactive effects of water table and precipitation on net CO2 assimilation of three co-occurring Sphagnum mosses differing in distribution above the water table. Global Change Biology 15(3), 680-691. DOI: https://doi.org/10.1111/j.1365-2486.2008.01724.x

Romanowicz, E.A., Siegel, D.I., Chanton, J.P. and Glaser, P.H. 1995. Temporal variations in dissolved methane deep in the Lake Agassiz Peatlands, Minnesota. Global Biogeochemical Cycles 9(2), 197-212. DOI: https://doi.org/10.1029/95GB00634

Salimi, S., Berggren, M. and Scholz, M. 2021. Response of the peatland carbon dioxide sink function to future climate change scenarios and water level management. Global Change Biology 27(20), 5154-5168.DOI: https://doi.org/10.1111/gcb.15753

Santoni, S., Garel, E., Gillon, M., Babic, M., Spangenberg, J.E., Bomou, B., Sebag, D., Adatte, T., Geldern, R.V., Pasqualini, V., Mattei, A. and Huneau, F. 2022 Mediterranean Peatland Water, Gas, and Soil content (Moltifau peatland, Corsica Island, France), Mendeley Data, V1. DOI: 10.17632/xt2gxmfc8z.1 (https://data.mendeley.com/datasets/xt2gxmfc8z).

Santoni, S., Garel, E., Gillon, M., Marc, V., Miller, J., Babic, M., Simler, R., Travi, Y., Leblanc, M. and Huneau, F. 2021. Assessing the hydrogeological resilience of a groundwater-dependent Mediterranean peatland: Impact of global change and role of water management strategies. Science of The Total Environment, 144721.DOI: https://doi.org/10.1016/j.scitotenv.2020.144721

Sebag, D., Disnar, J.-R., Guillet, B., Di Giovanni, C., Verrecchia, E.P. and Durand, A. 2006. Monitoring organic matter dynamics in soil profiles by 'Rock-Eval© pyrolysis': bulk characterization and quantification of degradation. European journal of soil science 57(3), 344-355. DOI: https://doi.org/10.1111/j.1365-2389.2005.00745.x

Sebag, D., Verrecchia, E., Cécillon, L., Adatte, T., Albrecht, R., Aubert, M., Bureau, F., Cailleau, G., Copard, Y. and Decaens, T. 2016. Dynamics of soil organic matter based on new Rock-Eval© indices. Geoderma 284, 185-203.DOI: http://dx.doi.org/10.1016/j.geoderma.2016.08.025

Siegel, D., Chanton, J., Glaser, P.H., Chasar, L. and Rosenberry, D. 2001. Estimating methane production rates in bogs and landfills by deuterium enrichment of pore water. Global Biogeochemical Cycles 15(4), 967-975.https://doi.org/10.1016/j.coal.2016.05.003

Turetsky, M.R., Bond-Lamberty, B., Euskirchen, E., Talbot, J., Frolking, S., McGuire, A.D. and Tuittila, E.S. 2012. The resilience and functional role of moss in boreal and arctic ecosystems. New Phytologist 196(1), 49-67. DOI: https://doi.org/10.1111/j.1469-8137.2012.04254.x

van Geldern, R., Schulte, P., Mader, M., Baier, A. and Barth, J.A. 2015. Spatial and temporal variations of pCO2, dissolved inorganic carbon and stable isotopes along a temperate karstic watercourse. Hydrological Processes 29(15), 3423-3440.DOI: https://doi.org/10.1002/hyp.10457

Vile, M.A., Bridgham, S.D. and Wieder, R.K. 2003. Response of anaerobic carbon mineralization rates to sulfate amendments in a boreal peatland. Ecological Applications 13(3), 720-734. DOI: https://doi.org/10.1890/1051-0761(2003)013[0720:ROACMR]2.0.CO;2

Weston, D.J., Timm, C.M., Walker, A.P., Gu, L., Muchero, W., Schmutz, J., Shaw, A.J., Tuskan, G.A., Warren, J.M. and Wullschleger, S.D. 2015. Sphagnum physiology in the context of changing climate: emergent influences of genomics, modelling and host-microbiome interactions on understanding ecosystem function. Plant Cell Environ 38(9), 1737-1751. DOI: https://doi.org/10.1111/pce.12458

Wieder, K., Canadell, J., Limpen, J., Moore, T., Roulet, N. and Schaepman-Strub, G. 2007. Peatlands and the carbon cycle: From local processes to global implications. Eos, Transactions American Geophysical Union 88(29), 295-295. DOI: https://doi.org/10.1029/2007EO290005

Wilson, R., Hopple, A., Tfaily, M., Sebestyen, S., Schadt, C., Pfeifer-Meister, L., Medvedeff, C., McFarlane, K., Kostka, J. and Kolton, M. 2016. Stability of peatland carbon to rising temperatures. Nature Communications 7(1), 1-10. DOI: https://doi.org/10.1038/ncomms13723

Yu, Z.C. 2012. Northern peatland carbon stocks and dynamics: a review. Biogeosciences 9(10), 4071-4085. DOI: https://doi.org/10.5194/bg-9-4071-2012

List of Figures (color should not be used for any figures in print)

Fig. 1: (A) Peatland surface (km²) in Mediterranean countries using data from Joosten (2009). (B) Wetlands in Corsica including Alpine peatlands and the Moltifau peatland. (C) Lithology, hydrogeology, and sampling network of the Moltifau peatland pilot site. (D) Schematic cross section of the peatland's hydrogeological functioning, with a particular focus on river water, colluvium, and granite groundwater mixing all together within the alluvial aquifer supplying the peatland.

Fig. 2. Fig. 2. Boxplot of hydrochemistry and isotope signatures for all peatland water and alluvial groundwater samples (median, quartiles, minimum, and maximum; n = 5 or n = 9 for each variable corresponding to peatland water and alluvial groundwater samples, respectively). Data were analysed with R statistical software (https://www.r-project.org/). The influence of seasons and waterbodies (alluvial groundwater or peatland water) was analysed with a two-way ANOVAs following Fisher LSD (least significant difference) test ($p < 0.05$). Different letters indicate significant changes between the seasons and waterbodies for each parameter..

Fig. 3. Keeling plots based on peatland CO_2 content and $\delta^{13}C_{CO2}$ values (A); Miller-Tans plots for alluvial groundwater (B) and peatland water based on DIC and $\delta^{13}C_{DIC}$ values. Regression lines and equations colours refer to the season. Their slope determines the $\delta^{13}C$ value of the unknown DIC source.

Fig. 4. Peat total, organic, and inorganic carbon contents deduced from CHN contents and I and R-indexes computed from Rock-Eval® thermal analysis parameters.

Fig. 5. DIC, DOC, DO, and $\delta^{13}C_{DIC}$ variations if alluvial, colluvium, granite, river, peatland and its outlets water samples.

List of Tables

Table 1: The $\delta^{13}C_{DIC}$ values of the peatland water samples are compared to the modelled $\delta^{13}C_{DIC}$ obtained from weighted means of the measured $\delta^{13}C_{DIC}$ in each water body supplying the alluvial aquifer ($\delta^{13}C$ standard error is less than 10%) and the mixing proportions from Santoni et al. (2020).

	Sample	Peatland $\delta^{13}C_{DIC}$ MEASURED	Peatland $\delta^{13}C_{DIC}$ COMPUTED (EMMA)	MEASURED - COMPUTED	10% error (from both $\delta^{13}C_{DIC}$ and EMMA analysis)	Interpretation
Summer	T1	-16.3	-16.9	0.6	3.3	Hypothesis validated
	T2	-17.6	-24.6	7.0	3.5	Input of enriched $^{13}C_{DIC}$
	T4	-13.1	-23.2	10.1	2.6	
	T5	-13.9	-26.2	12.4	2.8	
	T6	-13.0	-26.0	13.0	2.6	
Fall	T1	-9.6	-17.2	7.6	1.9	
	T2	-15.3	-17.2	1.9	3.1	Hypothesis validated
	T4	-17.0	-17.2	0.1	3.4	
	T5	-17.6	-17.2	-0.4	3.5	
	T6	-18.1	-17.2	-0.9	3.6	
Winter	T1	-18.8	-17.4	-1.3	3.8	
	T2	-16.7	-17.4	0.7	3.3	
	T4	-18.2	-17.3	-0.9	3.6	
	T5	-17.7	-17.3	-0.4	3.5	
	T6	-18.7	-17.4	-1.3	3.7	
Spring	T1	-13.7	-18.7	5.0	2.7	Input of enriched $^{13}C_{DIC}$
	T2	-18.4	-18.7	0.3	3.7	Hypothesis validated
	T4	-17.1	-18.1	1.0	3.4	
	T5	-14.4	-18.6	4.1	2.9	Input of enriched $^{13}C_{DIC}$
	T6	-16.4	-18.7	2.3	3.3	Hypothesis validated

Fig. 1

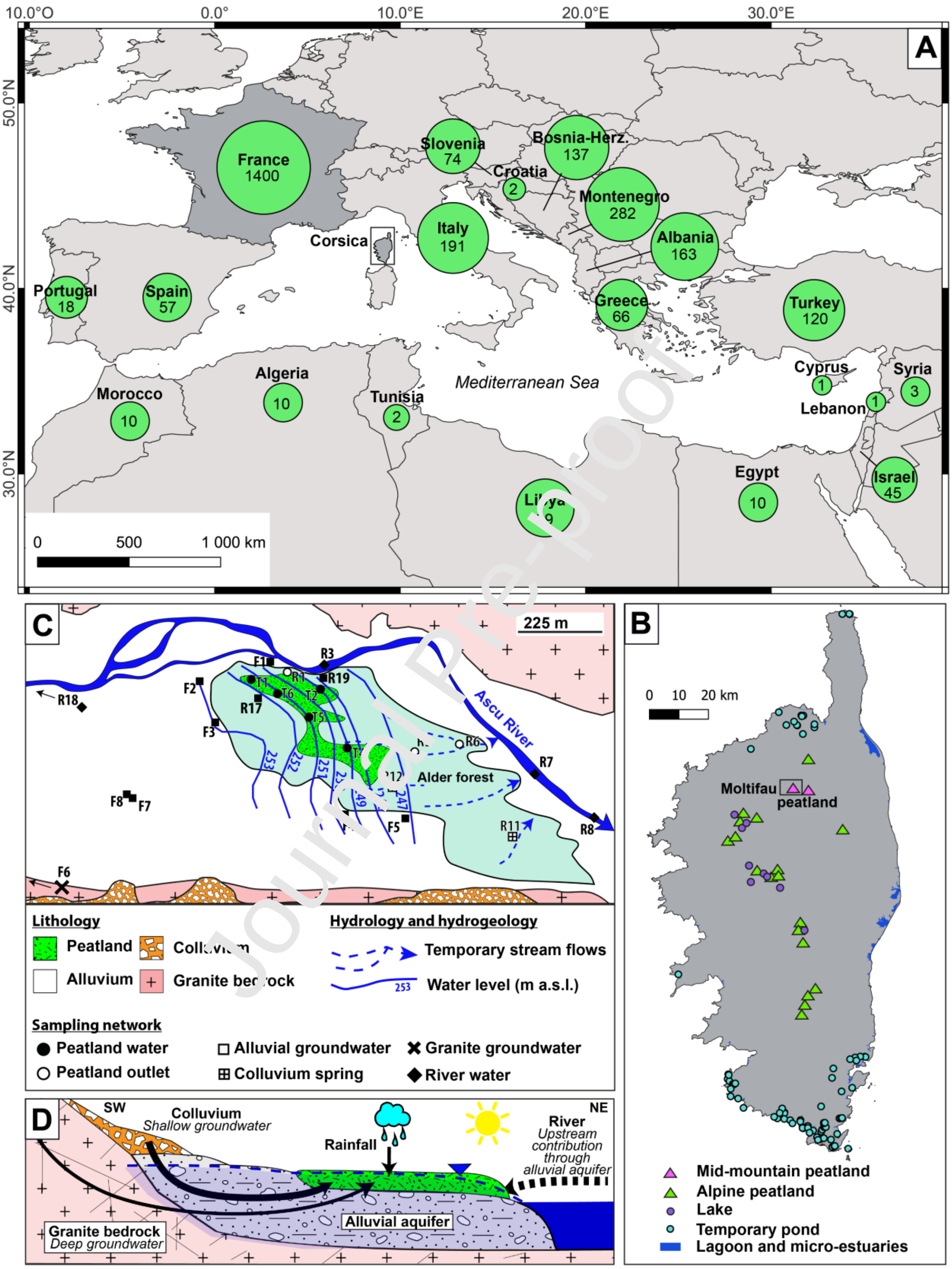
10.0°O
0.0°
10.0°E
20.0°E
30.0°E
50.0°N
40.0°N
30.0°N
A
France 1400
Slovenia 74
Bosnia-Herz. 137
Croatia 2
Montenegro 282
Italy 191
Albania 163
Corsica
Portugal 18
Spain 57
Greece 66
Turkey 120
Mediterranean Sea
Algeria 10
Morocco 10
Tunisia 2
Cyprus 1
Syria 3
Lebanon 1
Egypt 10
Israel 45
Libya 9
0
500
1 000 km
C
225 m
Ascu River
F1
R1
R3
R19
T1
T6
T2
R17
T5
F2
R18
F3
R6
R7
Alder forest
R12
253
252
251
249
247
F8
F7
F5
R11
R8
F6
Lithology
Peatland
Colluvium
Alluvium
Granite bedrock
Hydrology and hydrogeology
Temporary stream flows
Water level (m a.s.l.)
Sampling network
Peatland water
Peatland outlet
Alluvial groundwater
Colluvium spring
Granite groundwater
River water
B
0 10 20 km
Moltifau peatland
Mid-mountain peatland
Alpine peatland
Lake
Temporary pond
Lagoon and micro-estuaries
D
SW
Colluvium
Shallow groundwater
Rainfall
NE
River
Upstream contribution through alluvial aquifer
Alluvial aquifer
Granite bedrock
Deep groundwater

Fig. 2

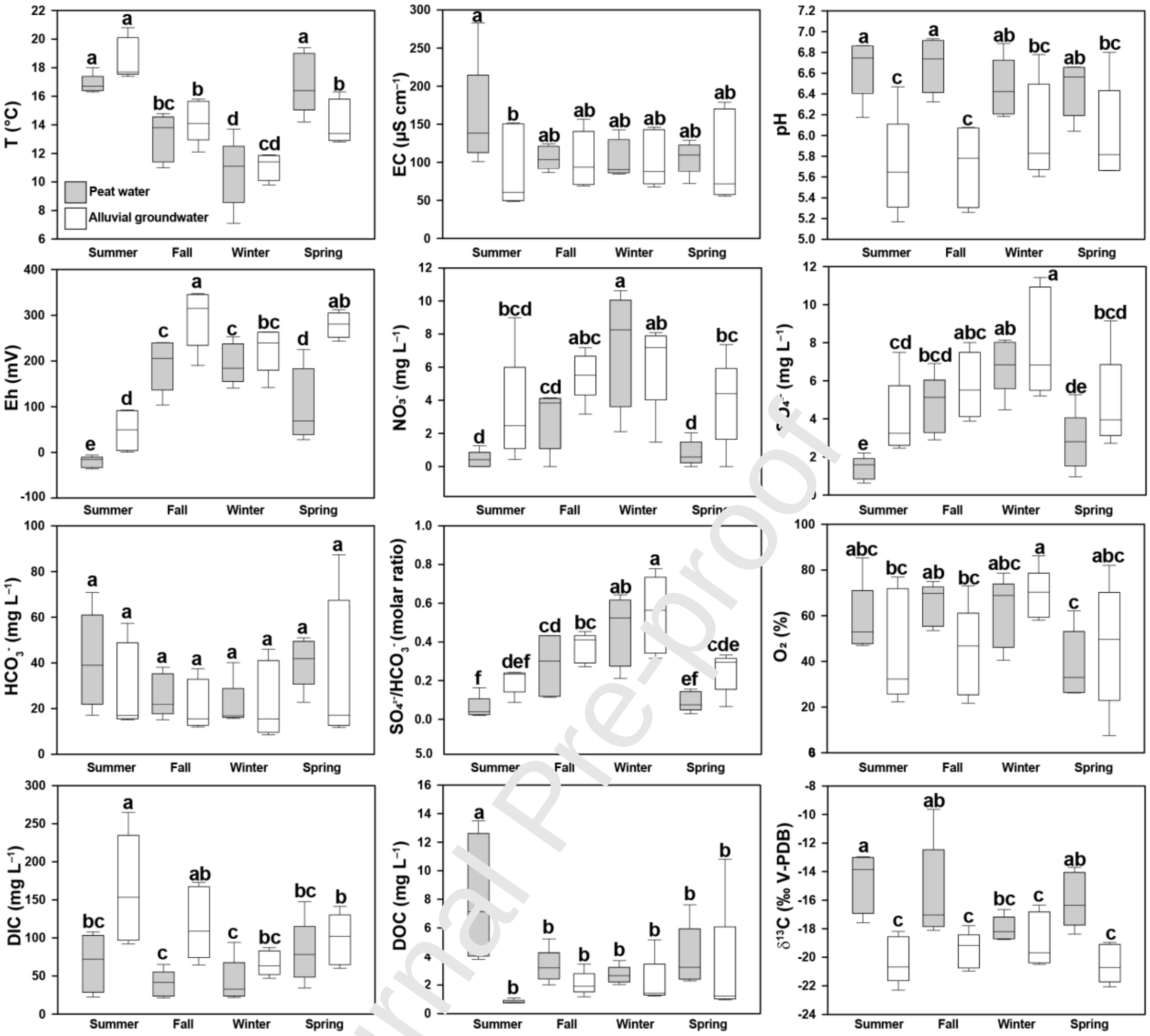
T (°C)
Peat water
Alluvial groundwater
EC (µS cm⁻¹)
pH
Eh (mV)
NO₃⁻ (mg L⁻¹)
SO₄²⁻ (mg L⁻¹)
HCO₃⁻ (mg L⁻¹)
SO₄²⁻/HCO₃⁻ (molar ratio)
O₂ (%)
DIC (mg L⁻¹)
DOC (mg L⁻¹)
δ¹³C (‰ V-PDB)
Summer
Fall
Winter
Spring

Fig. 3

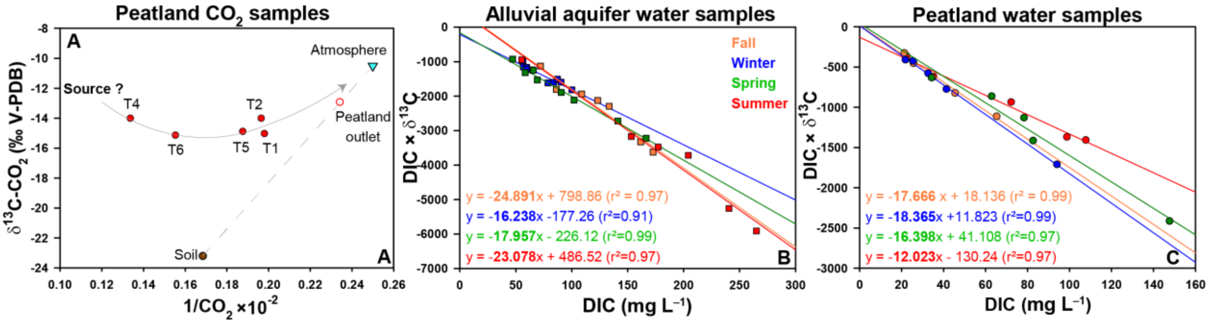
Peatland CO$_2$ samples
A
Atmosphere
Source ?
T4
T2
Peatland outlet
T6
T5
T1
Soil
A
δ^{13}C-CO$_2$ (‰ V-PDB)
-8
-10
-12
-14
-16
-18
-20
-22
-24
0.10
0.12
0.14
0.16
0.18
0.20
0.22
0.24
0.26
1/CO$_2$ ×10^{-2}
Alluvial aquifer water samples
Fall
Winter
Spring
Summer
y = -24.891x + 798.86 (r² = 0.97)
y = -16.238x -177.26 (r²=0.91)
y = -17.957x - 226.12 (r²=0.99)
y = -23.078x + 486.52 (r²=0.97)
B
DIC × δ^{13}C
0
-1000
-2000
-3000
-4000
-5000
-6000
-7000
0
50
100
150
200
250
300
DIC (mg L^{-1})
Peatland water samples
y = -17.666 x + 18.136 (r² = 0.99)
y = -18.365x +11.823 (r²=0.99)
y = -16.398x + 41.108 (r²=0.97)
y = -12.023x - 130.24 (r²=0.97)
C
DIC × δ^{13}C
0
-500
-1000
-1500
-2000
-2500
-3000
0
20
40
60
80
100
120
140
160
DIC (mg L^{-1})

Fig. 4

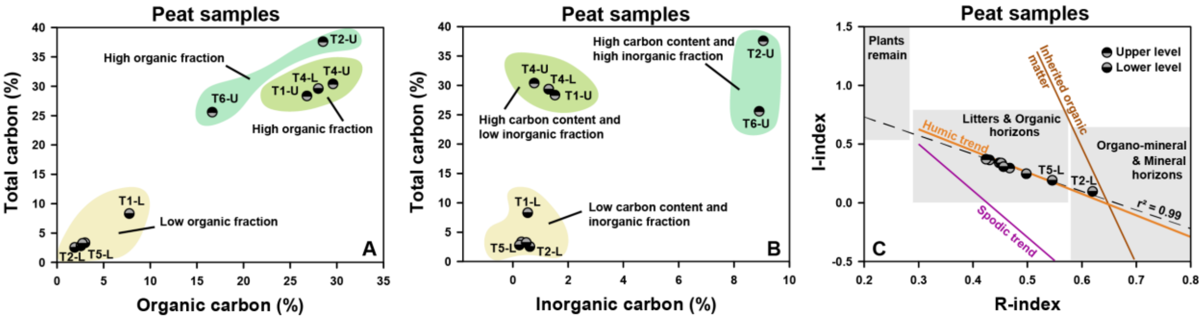
Peat samples
Total carbon (%)
Organic carbon (%)
T2-U
High organic fraction
T4-L
T4-U
T1-U
T6-U
High organic fraction
T1-L
Low organic fraction
T2-L
T5-L
A
Peat samples
Total carbon (%)
Inorganic carbon (%)
High carbon content and high inorganic fraction
T2-U
T4-U
T4-L
T1-U
High carbon content and low inorganic fraction
T6-U
T1-L
Low carbon content and inorganic fraction
T5-L
T2-L
B
Peat samples
I-index
R-index
Plants remain
Inherited organic matter
Upper level
Lower level
Litters & Organic horizons
Humic trend
Organo-mineral & Mineral horizons
T5-L
T2-L
r² = 0.99
Spodic trend
C

Fig. 5

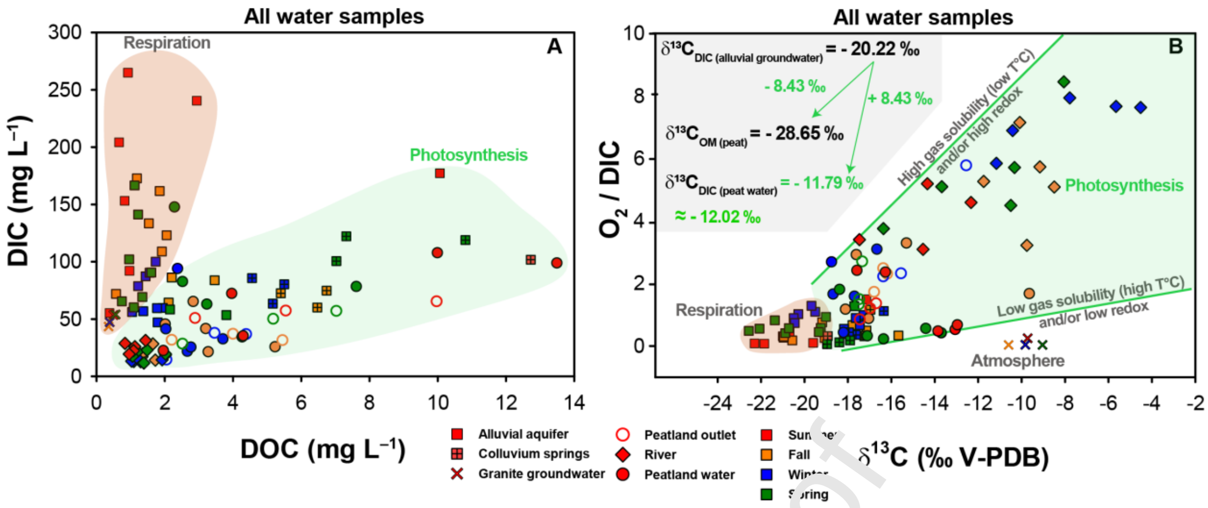
All water samples
A
Respiration
Photosynthesis
DIC (mg L⁻¹)
300
250
200
150
100
50
0
0
2
4
6
8
10
12
14
DOC (mg L⁻¹)
All water samples
B
δ¹³C DIC (alluvial groundwater) = - 20.22 ‰
- 8.43 ‰
+ 8.43 ‰
δ¹³C OM (peat) = - 28.65 ‰
δ¹³C DIC (peat water) = - 11.79 ‰
≈ - 12.02 ‰
High gas solubility (low T°C) and/or high redox
Photosynthesis
Respiration
Low gas solubility (high T°C) and/or low redox
Atmosphere
O2 / DIC
10
8
6
4
2
0
-24
-22
-20
-18
-16
-14
-12
-10
-8
-6
-4
-2
δ13C (‰ V-PDB)
Alluvial aquifer
Colluvium springs
Granite groundwater
Peatland outlet
River
Peatland water
Summer
Fall
Winter
Spring

Contributors

SS: Project design, field measurements, sampling, data interpretation, and manuscript writing. **EG**: Project design, field measurements, sampling, data interpretation, and manuscript corrections. **MG**: Data interpretation and manuscript corrections. **MB**: Sampling, analysis and methodology chapter corrections. **JES**: Data interpretation and manuscript corrections. **DS**: Data interpretation and manuscript corrections. **BB:** Analysis, data interpretation and manuscript corrections. **TA**: Data interpretation and manuscript corrections. **RvG**: Data interpretation and manuscript corrections. **VP**: Data interpretation and manuscript corrections. **AM**: Figures editing. **FH**: Project direction and design, field measurements, sampling, analysis, data interpretation, and manuscript corrections.

Declaration of interests

☐The authors declare that they have no known competing financial interests or personal relationships that could have appeared to influence the work reported in this paper.

☒The authors declare the following financial interests/personal relationships which may be considered as potential competing interests:

S. Santoni reports financial support was provided by Culletivittà di Corsica.

Graphical abstract

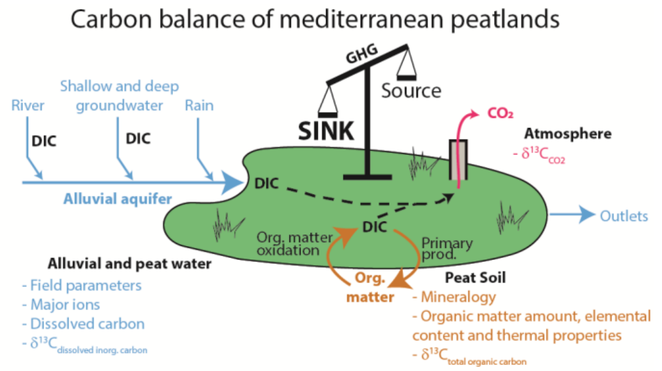

Highlights

- Seasonal investigations of hydrosphere, lithosphere, biosphere, and atmosphere.
- Isotope geochemistry approach suitable for peatland carbon balance studies.
- Groundwater support part or total peatland CO2 emissions.
- Groundwater maintains peatland carbon storage in changing climate conditions.
- Necessary to consider peatland hydrology to model global carbon balance.